Fermi National Accelerator Laboratory

FERMILAB-Pub-78/56-EXP
7551.247

(Submitted to Phys. Rev.)

SEARCH FOR SHORT-LIVED PARTICLES IN HIGH ENERGY NEUTRINO INTERACTIONS IDENTIFIED USING A HYBRID EMULSION-SPARK CHAMBER ARRANGEMENT

A. L. Read
Fermi National Accelerator Laboratory, Batavia, Illinois 60510 USA

and

G. Coremans-Bertrand, J. Sacton, and P. Vilain
Inter-University Institute for High Energies (ULB-VUB), Brussels, Belgium

and

A. Breslin and A. Montwill
University College, Dublin, Ireland

and

D. A. Garbutt
Imperial College, London, United Kingdom

and

E. H. S. Burhop, D. H. Davis, and D. N. Tovee
University College, London, United Kingdom

and

F. R. Stannard
Open University, Milton Keynes, United Kingdom

and

G. Blaes, R. Klein, and F. M. Schmitt
Institut des Sciences Exactes et Appliquées, Mulhouse, France

and

G. Baroni, F. Ceradini, M. Conversi, S. Di Liberto, L. Federici,
M. L. Ferrer, S. Gentile, S. Petrera, G. Romano, and R. Santonico
Istituto di Fisica, Universita di Roma and Sezione di Roma dell'INFN, Italy

and

G. Bassompierre, M. Jung, N. Kurtz, M. Paty, and M. Schneegans
Centre de Recherches Nucléaires, Université Louis Pasteur,
Strasbourg, France

June 1978

FERMILAB-Pub-78/56-EXP

SEARCH FOR SHORT-LIVED PARTICLES IN HIGH ENERGY NEUTRINO INTERACTIONS IDENTIFIED USING A HYBRID EMULSION-SPARK CHAMBER ARRANGEMENT

A. L. Read
Fermi National Accelerator Laboratory, Batavia, Illinois, USA

G. Coremans-Bertrand, J. Sacton and P. Vilain
Inter-University Institute for High Energies (ULB-VUB),
Brussels, Belgium

A. Breslin and A. Montwill
University College Dublin, Ireland

D. A. Garbutt
Imperial College, London, UK

E. H. S. Burhop, D. H. Davis and D. N. Tovee
University College London, UK

F. R. Stannard
Open University, Milton Keynes, UK

G. Blaes, R. Klein and F. M. Schmitt
Institut des Sciences Exactes et Appliquées, Mulhouse, France

G. Baroni, F. Ceradini, M. Conversi, S. Di Liberto, L. Federici,
M. L. Ferrer, S. Gentile, S. Petrera, G. Romano and R. Santonico
Istituto di Fisica, Universita di Roma and
Sezione di Roma dell'INFN, Italy

G. Bassompierre, M. Jung, N. Kurtz, M. Paty and M. Schneegans
Centre de Recherches Nucléaires, Université Louis Pasteur,
Strasbourg, France

ABSTRACT

Seventeen litres of nuclear photographic emulsion have been exposed to the wide-band neutrino beam at Fermilab. Tracks of secondaries from neutrino interactions in the emulsion were observed in a wide-gap spark chamber and a system of narrow-gap spark chambers and counters down beam. From measurements on the tracks in the wide-gap chamber the positions of vertices from which the secondaries diverged were predicted and 37 neutrino interactions in emulsion were located. Factors affecting the efficiency of location of events searched for (~20% in this experiment) are assessed and conclusions drawn about means of optimizing the design of experiments employing emulsion hybrid techniques. In one of the interactions a secondary track gave rise to three tracks after a distance of 182 μm. Further measurements made on this event do not alter the previous conclusion of its most likely interpretation as the decay of a short-lived particle of life-time $\sim 6 \times 10^{-13}$ s.

I. INTRODUCTION

Charmed hadrons and heavy leptons of masses near 2 GeV/c^2 for which there is now very strong experimental evidence are expected to have mean lifetimes in the range 10^{-12} to 10^{-14} s. Direct observation of the production and subsequent decay of particles with such lifetimes is only possible at present in photographic emulsion with its high spatial resolution (of the order of 1 μm). The study of high energy neutrino interactions using both bubble chambers and electronic detection and analysis suggests that charmed hadrons are produced in at least a few percent of these.[1]

The photographic technique suffers from the disadvantage of prohibitively long scanning times when studying processes with small cross sections. By combining it with other techniques (spark chamber, bubble chamber) it is possible to detect emitted secondary particles and to use these to predict the position of the interaction from which they have come, thus reducing by orders of magnitude the volume of emulsion to be scanned.

The feasibility of this method has been demonstrated earlier.[2] This paper describes a search for short-lived particles in emulsion exposed in the wide-band neutrino beam at Fermilab. A system of spark chambers and counters was used to select and locate successfully 37 such neutrino interactions in emulsion, in one of which a likely example of a short-lived charmed particle was observed.[3] This experiment has demonstrated the great potentialities of this technique especially in view of the practicability of a substantial improvement in the accuracy of prediction of the position of the interaction.

An account of the results of the experiment is presented in this paper with particular emphasis on technical aspects of the arrangement, testing and operation of the apparatus, on the analysis of the spark chamber photographs and the method of vertex reconstruction, and on the scanning and interaction location in the emulsion. A discussion of the characteristics of the interactions located is followed by a brief discussion of further measurements on the event that has been interpreted as a likely example of the decay of a charmed particle. Conclusions are drawn concerning factors that should influence the design of future hybrid experiments using photographic emulsion.

II. EXPERIMENTAL CONDITIONS AND SET-UP

The experimental set-up consisted basically of six emulsion stacks associated with a wide gap (WG) spark chamber which enabled the location of high energy neutrino interactions in the emulsion. A number of scintillation counters provided a trigger system for selecting events of the desired type. An electromagnetic shower detector and a somewhat rudimentary muon identifier helped in the analysis of the interactions observed. Figure 1 shows the arrangement of the apparatus, which was situated approximately 50 m behind the 15' bubble chamber in the Fermilab neutrino beam line.

A. The Emulsion Stacks

Some 1900 pellicles of Ilford K5 emulsion, each 600 μm thick, were assembled in six clamps and the edges accurately milled to form six approximately equal blocks of emulsion of dimensions 19 x 20 x 7.3 cm^3 (i.e., a volume of 16.6 ℓ). The clamps were located to an accuracy of ~0.1 mm on an aluminum alloy frame which was mounted so that the short dimension of each stack was parallel to the neutrino beam direction. The distance between the down-beam face of the emulsion stack and the first electrode of the WG spark chamber was ~20 cm.

The stacks were assembled at Fermilab immediately prior to the exposure, the pellicles being shuffled to reduce the background of cosmic ray tracks that "follow through" from one pellicle to another. After milling they were sealed with adhesive tape to minimize effects due to humidity. After the experiment the stacks were taken to CERN, disassembled, gridded and processed. Since preliminary tests had revealed that normal processing on glass of these batches of emulsion gave severe problems of adhesion, leading to an unacceptable number of bubbles between emulsion and glass, the pellicles were processed free, before mounting on the treated glasses.

B. Track Chambers, Counters and Electronics

1) Track Chambers

The construction of the WG spark chamber with two 15 cm gaps and a sensitive area of 100 x 80 cm^2 is shown in Fig. 2. Two

earthed 5 mm thick, rectangular aluminum plates (142 x 122 cm^2) were placed symmetrically on either side of a common central high voltage electrode consisting of a 3 mm thick rectangular plate (114 x 92 cm^2) and were held off from it by means of two rectangular frames constructed from plexiglass sheets 15 cm wide and 2 cm thick.

The three plates and two plexiglass frames were pressed together by a mechanical structure which also supported a box containing a 12-stage Marx high voltage (HV) generator and filled with N_2 at high pressure. The voltage pulse applied to the central electrode from the generator has a voltage of ~100 kV and length ~300 ns.

The WG spark chamber itself contained Neogal (70% Ne, 30% He) and had a memory time of ~20 μs, large compared to the total delay time of the triggering pulse (~500 ns). A feature of this design is the compact shielding of the WG spark chamber and generator which eliminated interference with nearby electronics, while the relative dimensions of the three electrodes guaranteed homogeneity of the electric field in the useful volume.

Of five narrow-gap (NG) spark chambers (C_{0-4}), four formed an integral part of the shower detector (SD) while the other (C_o), placed upstream with respect to the emulsion stack, defined those charged incoming particles which appeared in the other chambers but were uncorrelated in time with the electronic trigger signal (Sect. II.B.2). The chambers C_{1-4} proved helpful, in the absence of more refined methods of momentum measurement, by enabling tracks of slow

particles absorbed or scattered in the lead of the SD to be recognized and consequently discarded in the vertex prediction computations.

2) Trigger Signal

The veto counter, V, consisted of four scintillators covering an area of ~2.2 m^2. Counters S_{1-4} were plastic scintillators, 2 cm thick, each viewed by four photomultipliers arranged to ensure the efficient, uniform light collection required for the pulse height analysis of the SD (Sect. II.B.3). The pulses from all scintillation counters were shaped at ~ 40 ns. The signal used to trigger all spark chambers was $\bar{V}\ S_o\ S$ (MG) where S means time coincidence in at least three of S_{1-4} and (MG) is the "machine gate" signal, largely overlapping the 20 μs spill-out time.

3) The Shower Detector (SD)

This consisted of five Pb plates, L_{1-5}, of thicknesses 3, 3, 6, 10, 10 mm respectively, associated with the four counters S_{1-4} and the four NG chambers C_{1-4}, in the arrangement shown in Fig. 1. The NG chambers each had six 1 cm gaps and their effective transverse dimensions were 1 x 1 m^2. The pulse height was digitized and recorded on the spark chamber film by means of LEDs.

4) The Muon Identifier

Muons in the forward direction of momentum $\geq$ 2 GeV/c could penetrate the lead wall, 135 cm thick, and register counts in the scintillation counter hodoscope, S_μ. This consisted of ten partially overlapping counters of dimensions 61 x 122 x 2 cm^3, disposed in three parallel planes and overlapped in such a way as to

define 26 different regions covering a total area of 4.3 m^2. The hodoscope pattern was recorded on the spark chamber film.

The muon identifier provided a signature of the charged current ν interaction events and provided the possibility, in favorable cases, of identifying the muon track coming from the interaction. By studying a sample of completely reconstructed single tracks through the whole apparatus the totel accidental coincidence rate was estimated as ~5%. The hadronic punch-through from events in the emulsion was negligible.

C. The Operating Conditions During Data Taking

The total number of protons of momentum 400 GeV/c on target during the usual "two horn" running of the wide band (WB) ν beam was 6.7×10^{17}. In addition a small number of interactions was contributed during a "bare target" ν run and a short "two horn" WB $\bar{\nu}$ beam run.

The following coincidence rates were recorded in the main run when the accelerator was operated with 10^{13} protons of energy 400 GeV per burst on the neutrino target:

(1) $\bar{V} S_o S$ (MG): ~0.1 per burst

(b) $\bar{V} S_o S S_\mu$ (MG): ~0.05 per burst

(c) $V S_o S S_\mu$ (MG): ~1 per burst.

Comparison of rates (b) and (c) indicates that at most 5% of the muons traversing the apparatus escaped the veto counter, V. Cosmic rays contributed less than a fraction 10^{-3} to the trigger rate during the 20 μs spill.

D. Tests and Calibration Measurements

Before transportation to Fermilab the WG chamber and SD were assembled at CERN and exposed to monoenergetic electrons of known momenta from 1-12 GeV/c derived from a γ-ray "test beam" of the 28 GeV proton synchrotron, enabling the SD to be calibrated and the WG chamber performance studied. The calibration showed the total pulse height of the scintillation counters to be approximately proportional to the energy of the incoming electrons in the range 1-12 GeV. The energy of the shower could be estimated to an accuracy of ~25%.

For single particles entering the chamber at an angle θ to the electric field direction (i.e., parallel to the beam line) less than 35°, the chamber efficiency was nearly 100%. Even for electromagnetic showers with up to ~20 particles the tests showed that efficiencies between 95-100% for θ up to 30° were obtainable. The track luminosity, however, decreased rapidly for increase of θ. Optimum spatial resolution consistent with high multitrack efficiency led to a choice of operating conditions (shape of HV pulse, gas mixture, gas flow etc.) such that sparks had a diameter of ~1.5 mm for $\theta = 20^{\circ}$. Under these conditions measurements on the tracks gave dispersions Δx, $\Delta y \sim \pm 0.2$ mm, $\Delta\theta \sim \pm 3$ mr, where x, y are the coordinates of the track center in directions perpendicular to the electric field.

During the actual run at Fermilab acceptable operating conditions were generally maintained but there was a much more rapid

decrease of efficiency for tracks with $\theta > 20^{o}$, while usually the luminosity of the tracks in the gap nearest the emulsion stack was weaker than that in the other gap, due possibly to a small difference of gas composition between the two gaps.

III. PREDICTION of ν INTERACTION POSITION FROM SPARK CHAMBER FILM SCAN AND MEASUREMENT

A. The Optical Recording System

A camera with a single objective (f = 300 mm), at a distance large enough (~12 m) to provide sufficient field depth, produced on the same film images of the sparks in a direct view and a 90^{o} stereo view from mirrors above the WG and NG chambers. Two sets of 24 fiducial marks for horizontal and vertical positions, produced by LEDs located in boxes behind small holes, 0.5 mm in diameter, were photographed on the same film. These boxes were rigidly clamped to the stack holders. The positions of the fiducial marks relative to each of the emulsion stacks mounted on the supporting frame were measured to ~0.2 mm by the Fermilab Survey Group before and after the exposure. In the photograph of an actual event shown in Fig. 3 the fiducial marks and LED displays can be seen.

B. Scanning of the Spark Chamber Film

The candidates for ν interactions in the emulsion were selected on the scanning table according to the following criteria:

(a) At least two tracks were visible in the WG chamber converging to a point inside the emulsion.

(b) Tracks appearing also in the veto chamber were discarded. The different luminosities in the WG chamber of tracks from a given event were used to correlate the tracks between the two views. The pattern of sparks in the NG chambers was used to resolve ambiguities in correlation in a number of cases.

C. Space-Film Correspondence and Track Reconstruction

The correspondence between the coordinates (x, y, z) of a point in space and the coordinates (η,δ) of its image on the film was represented in the usual way by the projective expressions

$$\eta = \frac{C_1x + C_2y + C_3z + C_4}{C_9x + C_{10}y + C_{11}z + C_{12}}, \quad \delta = \frac{C_5x + C_6y + C_7z + C_8}{C_9x + C_{10}y + C_{11}z + C_{12}}$$

for each of the two views, z being along the beam direction, x in the plane of the emulsion pellicles and y perpendicular to that plane. The coefficients C_i were overdetermined from the known positions of the 24 fiducial marks. The accuracy of reconstruction of a point in space from measurements on the film was typically 0.1 - 0.2 mm.

A maximum of ten points per gap per view was measured for each track. The tracks were reconstructed as straight lines. An independent fit was made for each gap. Figure 4(a) shows the average dispersion of the reconstructed points about the fitted space track for a sample of 200 tracks. Owing to electron drift in the electric field which was in opposite directions in the two halves of the WG

chamber there was a displacement D between the reconstructed tracks in the two gaps which depended on the angle between the particle and electric field directions. The data of Fig. 4(b) were fitted by the expression

$$D_{x,y} = (-9.5 \pm 1.0) \tan W_{x,y} \text{ (D in mm)},$$

W_x, W_y being respectively the projected angles in the (x, z) and (y, z) planes between the track and the z axis. A correction of half this magnitude was applied when a track was measurable in only one gap.

D. Vertex Reconstruction

For each candidate interaction, all tracks approximately pointing back to a vertex in the emulsion were measured.

Two methods have been used to estimate the position of this vertex. In one method the tracks in each view were constrained separately to pass through a point and the corresponding space point calculated. The other method involved direct space reconstruction of each track, followed by a fit constraining these tracks to diverge from a point in space. In either method, after a first approximation to the vertex was found, each track was weighted inversely according to its estimated measurement errors and its perpendicular distance from the approximate vertex position in order to give a corrected vertex prediction.

Figure 4(c) shows typical values of the perpendicular distance between the reconstructed vertex and the tracks used in the reconstruction. A combination of both methods was used to define the volume to be searched.

IV. SCANNING AND EVENT LOCATION IN EMULSION

A. Method of Scanning

An area scan was carried out under ~ x 300 magnification over a volume (typically ~1 cm^3) of emulsion indicated by the reconstruction calculations(*). All interactions were noted and carefully examined under higher magnification (~ x 750) for tracks of minimum ionization in the forward hemisphere. The directions of such tracks were measured with an accuracy of ~ $\pm$ 0.5^o in azimuth and ~ $\pm$ 1^o in dip.

B. Criteria for Identification of Neutrino Interactions

Stars were accepted as candidates for neutrino interactions if they:

(*) The volume searched for each predicted vertex extended typically over about two standard deviations of the x, y and z coordinate predictions. This is subsequently referred to as the "search volume" or, when specified in terms of the corresponding total area of emulsion pellicles, each ~0.6 mm thick, as the "search area". It is clearly a rather loosely defined quantity.

(a) contained no minimum ionization tracks coming from the beam direction.

(b) consisted of tracks that "followed through" from pellicle to pellicle;

(c) contained at least two tracks of minimum ionization with azimuth and dip angles, measured in emulsion, agreeing within $\pm 2^{o}$ with the corresponding angles observed in the WG chamber (**).

Once a candiate satisfying these criteria was found, the scanning for that interaction was terminated. All secondary minimum tracks from the interaction were followed to the edge of the stack if possible. Special attention was paid to any sudden changes in direction which could be the result of a decay in flight. A search was made also for possible decays of neutral particles by carefully scanning under high magnification for at least 2 mm in a forward cone of semi-vertical angle 45^{o}.

(**) Due to the curvature of the emulsion surface near the edges of the pellicles, dip measurements in a few events showed a systematic variation from the predicted angles. The criterion (c) was then adjusted by requiring the relative values of these angles to be in agreement.

C. Background in the Emulsion

Most of the observed stars in the emulsion were due to cosmic rays and neutrons. Despite the long period between pouring and processing of these emulsions the background was acceptable. The minimum ionization tracks from background stars were found to be uniformly distributed in angle, at least over a cone of semi-vertical angle 30° with the beam direction. The number of background stars containing at least two minimum tracks within this cone was ~ 0.25 cm^{-2} while the number having at least one minimum track in the forward (beam) direction was ~ 3.5 cm^{-2}.

D. The Evidence that the Events Located are Neutrino Interactions

From these background numbers and the areas scanned in locating interactions it can be concluded that for most candidates the chance of a background interaction fortuitously satisfying the above criteria ranges from 10^{-4} to 10^{-7}. Overall it is estimated that the chance of one of the 37 ν interaction candidates being background is $\sim 6.5 \times 10^{-3}$, 80% of this probability being contributed by one particular event. An area of 328 cm^2 of emulsion was scanned for the 37 events located (8.86 cm^2 per event). An additional area of 5360 cm^2 was scanned fruitlessly for 157 further apparent events measured in the WG spark chamber. The failure to find any candidates for these further demonstrates the small chance of a background interaction simulating a candidate.

1) Correlation between predicted and observed positions of neutrino interaction candidates

Figure 5 shows the distribution of the quantities Δx, Δy, Δz, defined as $\Delta x = \{x(\text{observed}) - x(\text{predicted})\}$, etc. x and z are given in mm while y is expressed in number of pellicles (standardized to a mean thickness of 0.6 mm). The distributions do not exactly center at zero, possibly reflecting small systematic errors in the predictions, ($\overline{\Delta x} = 0.70$ mm, $\overline{\Delta y} = -1.3$ mm, $\overline{\Delta z} = -3.35$ mm). There is a suggestion in particular of a systematic error in y values for the upper (A, B, C) stacks while the y distribution for the lower stacks (D, E, F) centers round zero. This could possibly account for the distribution between stacks of the numbers of events found (13 in A, B, C; 24 in D, E. F).

The RMS dispersions about the means were $\sigma_x = 1.16$ mm, $\sigma_y = 1.36$ mm, $\sigma_z = 9.78$ mm.

2) Correlation of directions of secondaries with predictions

Figure 6 shows the distributions of differences between the observed and predicted azimuthal and dip angles, $\Delta\theta$, $\Delta\phi$. The RMS deviations are

$$\{\overline{(\Delta\theta)^2}\}^{1/2} = 1.0^{\circ};\ \{\overline{(\Delta\phi)^2}\}^{1/2} = 1.2^{\circ},$$

in reasonable agreement with the estimated measurement accuracy. Where an appreciable change of direction has occurred between the interaction and the exit point of the particles from the stack the latter direction has been used.

3) The distribution of tracks of minimum ionization

Figure 7 shows the number distribution of shower tracks (n_s) in the 37 events located. It is compared with the number distribution of particles that leave the chamber after emission from neutrino charged—current interactions produced in the CERN cryogenic bubble chamber, BEBC, filled with an H_2 - Ne mixture and exposed to the CERN WB neutrino beam which has a spectrum comparable with that of the Fermilab WB neutrino beam.(*) The method of vertex prediction in the present experiment discriminates against events of low multiplicity. A minimum of two tracks is needed in order to make any vertex prediction. The two distributions of Fig. 7 are therefore normalized to the same total number of events having $n_s > 3$ where they are compatible.

4) Information from the muon identifier

The muon identifier was only operational for 29 of the 37 events found. At least one counter in the muon hodoscope was triggered in 22 of these 29 events. Unambiguous correlation with a particular track observed in the emulsion was found for 15 of the events.

It can be concluded from the correlations between the predicted and observed positions of the interactions, between the predicted and observed directions of the tracks and from the characteristics of the interactions, that not only are the events

(*) We are grateful to the BEBC WA24 collaboration and especially to Drs. H. Bingham and T. W. Jones for supplying us with this distribution.

observed in emulsion those predicted from the WG spark chamber observations but that their characteristics are similar to those expected for neutrino interactions.

V. EFFICIENCY OF FINDING INTERACTIONS

The efficiency of finding neutrino interactions in emulsion using a hybrid technique has to be assessed from the points of view of the area of emulsion that has to be scanned to locate an event and the proportion of total events located.

A. Area of Pellicles Scanned

Figure 8 shows the distribution of the areas scanned in searching for the 37 events found. In all, 328 cm^2 were scanned in searching for these events.

No magnetic field was included in the experimental arrangement used. The meagre knowledge available of secondary particle momenta made it difficult to differentiate between good vertex predictions based on the intersection of tracks of high momentum particles and inexact predictions using scattered particles of low momentum. It led to uncertainty in the estimate of errors in vertex prediction and thence in prescribing the area to be searched.

The search for events for which vertex predictions appeared satisfactory was extended at least up to ~30 cm^2. For some particular events the scanned areas were much larger. In order to combine all the results in drawing meaningful conclusions about the

area of scan needed to locate events a cut-off in this area of 30 cm^2 has been applied. Only two of the 37 events found would have been missed if this cut-off had been applied systematically to all the events.

Table I shows the total area scanned per event found with this cut-off applied. The events found are distributed between four equal zones in z, the coordinate in the beam direction, zone 1 being closest to the WG chamber. It is evident that the scanning effort required to find an event is more than twice as great in zone 4 as in zone 1. The average path in the emulsion of secondaries from interactions in zone 4 is ~6 cm compared with ~1 cm from zone 1.

B. Distribution of Coordinates of Events

Figure 9 shows the x and z grid co-ordinates of each of the 37 events located, irrespective of their emulsion plate numbers. The distribution is uniform in x but in the z direction 38% of the events have been found in zone 1 and only 11% in zone 4.

C. Effect of Multiple Scattering and Nuclear Interactions of Secondary Particles on the Efficiency of Finding Vertices

The distributions in area scan (Table I) and in event co-ordinates (Fig. 9) illustrate the importance, for accuracy of vertex reconstruction, of multiple scattering and nuclear interactions of secondaries before emerging from the emulsion. Nuclear interactions of secondaries, observed in one quarter of the ν interactions in emulsion, contribute tracks that in many cases cannot be rejected in the reconstruction of the vertex. Such

secondary tracks increase the uncertainty of the vertex prediction and thence of the search area. The NG spark chammers of SD provided some limited information on momenta, enabling the scattering of secondaries to be estimated from the line of sparks in the series of chambers separated by lead plates of total surface density 47 g cm^{-2} . For pions the minimum momentum required to penetrate the system was ~200 MeV/c, while the absence of appreciable scattering indicated a lower limit of momentum of ~500 MeV/c. Such unscattered tracks are defined as "straight" in the subsequent discussion. Table II which gives the relative frequency of such "straight" tracks reveals a correlation between their presence and the efficiency of locating an event. In the sample of 138 predictions for which data are available the event location efficiency was 60% greater for events with two or more "straight" tracks than for the whole sample.

D. Depth Distribution in Pellicles of Events Located

Figure 10 gives the distribution of the depth in the pellicles of the events found. It suggests some loss of events near the bottom surfaces as could be expected since in many cases quite heavy surface fog affected visibility, particularly near the bottom of the pellicles.

E. Scanning Efficiency

No systematic rescan was made for ν interaction candidates. An estimate of the scanning efficiency made from two independent

scans of the same emulsion area for any stars containing more than one minimum track in the forward direction gave 80%. This estimate is relevant to stars containing black or grey prongs in addition to minimum ionization tracks. In high energy hadron interactions around 10% of the stars are "white" stars containing no black or grey prongs. The efficiency of finding "white" stars can be expected to be lower than for other stars. One "white" star was observed among the 37 interactions found, compared with an expected number of three or four (± 2), if one makes the plausible assumption that they occur in neutrino interactions in emulsion in about the same proportion as in hadron interactions.

F. The Proportion of Interactions Located

1) Estimate of total number of interactions

During most of this experiment the 15-Ft. bubble chamber was operating with a mixture of liquid Ne and H_2 (atomic ratio of Ne, 64%) in the same two-horn WB neutrino beam approximately 50 m up beam from the emulsion stacks. An estimate of the number of ν interactions in the emulsion can be obtained from the event rate observed in the bubble chamber[*] taking account of the relative n/p ratio, the spread of the ν beam and the actual running conditions. The estimate is 230 ± 70 including both charged and neutral current interactions. The large error quoted arises mainly from uncertainty in the radial dependence of the ν beam intensity. The

[*] We are indebted to Dr. M. Kalelkar for extracting these data and to Prof. C. Baltay for allowing us to use them.

comparable figure estimated from the ν spectrum and the total cross section for ν interactions on an isoscalar target is ~300, but this does not allow for the spread of the ν beam and could also be affected by targeting conditions. The number of interactions for which vertex predictions were made from the WG spark chamber was 194 and this number certainly includes some neutron interactions.

2) Estimate of loss factors in locating predicted interaction vertices in emulsion

(a) Loss of low multiplicity events

Figure 7 indicates a loss of low multiplicity events in emulsion compared with the bubble chamber results, as expected. The corresponidng loss factor for events with prong number ≤ 3 is $50/37 = 1.35 \pm 0.2$(*). This correction factor has to be applied both to the number of vertices predicted and to the number of interactions found.

(b) Loss due to finite scan volume

If the distribution of Fig. 9 is interpreted as reflecting the influence of multiple scattering and nuclear interactions on the vertex reconstruction accuracy and that in the absence of these effects the rate of finding events throughout the stack would have been the same as in zone 1, the loss factor is $(4 \times 14)/37 = 1.5 \pm 0.4$.

(*) Minimum ionization tracks in emulsion correspond to particles with $\beta \geq 0.7$. Tracks that cross 2 m of BEBC containing the Ne-H_2 mixture specified would correspond to protons with $\beta \geq 0.75$ or pions with $\beta \geq 0.95$. In Fig. 7 tracks of stopping particles have been excluded from the BC distribution. If they are included however, the loss factor calculated in the same way is 1.37.

(c) Emulsion scanning losses

Even under good observational conditions a scanning loss factor of 100/80 = 1.25 is implied by the estimated scanning efficiency (Sect. V.E). There is the additional scanning loss however, due to poor visibility of events near the bottom of the emulsion pellicle (Sect. V.D). If the distribution of Fig. 10 is due to this factor the correction factor can be estimated as (29/37) x (3/2) = 1.2 ± 0.2.

The difficulty of observing white stars leads to further losses. Assuming one would have expected four white stars instead of the one observed the correction factor is (37 + 3)/37 =1.1 ± 0.1. The overall emulsion scanning loss factor is then

$$1.25 \times 1.2 \times 1.1 = 1.65 \pm 0.35.$$

(d) Loss due to systematic error in location of stacks A, B, C

If this is responsible for a loss of events in these stacks the loss factor can be estimated as 2 x 24/37 = 1.3 ± 0.3 (Sect. IV.D.1 and Fig. 5(b)).

3) Comparison between the observed and expected number of events

Taking 230 ± 70 as the expected number of ν interactions the number of vertex predictions expected, allowing for the loss of low multiplicity events, is

$$230/1.35 = 170 \pm 50$$

Other losses arise from random vetoing due to the presence of an unrelated particle in V coincident with a ν interaction in emulsion, from inefficiency of counter electronics, or for events for which ambiguity in the spark chamber photographs makes vertex prediction very inaccurate or impossible. These losses are difficult to evaluate but could be about 10 or 20%, thus reducing the number of vertex predictions to ~ 140. This has to be compared with a total of 194 predictions actually made, including an unknown number of neutron interactions which, being of lower energy, will be located with lower efficiency. On the other hand the total number of neutrino interactions that would have been detected in the absence of scanning and systematic losses is $37 \times 1.5 \times 1.65 \times 1.3 = 119 \pm 47$.

Although the statistics are far too small to establish these estimates with great confidence there is no clear inconsistency between the number of events located, the number of "good" vertex predictions and the total number of ν interactions expected in the stack.

Taking 140 as the actual number of ν interactions that could have been found the overall location efficiency can be estimated in this experiment as

$$37/140 \approx 26\%$$

Expressed in terms of the 194 vertices actually looked for, the efficiency is nearer to 20% however.

VI. THE NEUTRINO INTERACTIONS LOCATED IN EMULSION AND THE EMISSION OF POSSIBLE SHORT-LIVED PARTICLES

The characteristics of the neutrino interactions located in the emulsion are summarized in Table III.

The multiplicity distribution of relativistic particles emitted from interactions in a comparable energy range is well known from bubble chamber measurements and has indeed been used (Fig. 7) to confirm the identification of interactions in emulsion. Almost all these relativistic particles are emitted within a forward cone of semi-vertical angle 30° while their emission in a backward direction is very rare. Figure 11 gives, for the 37 events located in emulsion, the distribution of the total angle between the shower particles and the neutrino beam direction.

The tracks of relativistic particles were followed until they interacted, decayed or left the stack. Nine definite examples of nuclear interactions were observed in following 405.7 cm of minimum ionization track. It is estimated that this included ~75 cm of muon track from charged current interactions so that the corresponding interaction length of secondary hadrons is 36.7 cm. The interaction length of pions in nuclear emulsion is 38.5 ± 0.5 cm. The average distance of each track followed was ~2 cm, corresponding to a flight time of 6×10^{-11} s. Decays of unstable particles after a

path of 6 μm (flight time ~2 x 10^{-14} s) should certainly have been seen.

Only one apparent decay (that from event 8/151) was observed, at a distance from the parent interaction of 182 μm (flight time ~6 x 10^{-13} s).[3] From the number of tracks of fast secondaries from ν interactions now followed the chance of the alternative explanation of this apparent decay as a nuclear interaction is 1 in 400, estimated on the basis described in Ref. 3. The event is discussed in Sect. VII.

The search for the decay of neutral particles extended 2 mm down beam from the interactions, within a cone of semi-vertical angle 30^{o}. None was observed.

Other information on neutrino interactions not obtainable from bubble chamber studies concerns the slower particles emitted, related more to the nuclear physics rather than the particle physics of the interactions. The slow particles ("black" tracks) are isotropically distributed (102 in the forward and 95 in the backward hemispheres), while the faster particles may remember slightly the direction of the incident neutrino (29 forward, 20 backward). Figure 12 show the range distribution of black and grey prongs from this sample, including only particles coming to rest in the emulsion.

The event 62/102 contains a short track (length 3 μm) of a hyper-fragment which decays non-mesonically. The energy release in the decay is consistent with its interpretation as a normal hyper-fragment.

VII. ANALYSIS AND INTERPRETATION OF THE EVENT IN WHICH A SHORT-LIVED DECAY CANDIDATE IS OBSERVED

Further measurements carried out since this event (8/151) was reported,[3] in an attempt to obtain a more detailed interpretation, are briefly described in this section.

A. Topology of the Event

On the basis of the correlation between emulsion observations and the spark chamber pictures the topology of the event is illustrated in Fig. 13. The conclusion of the earlier analysis was that in order to conserve momentum at the vertex B, at least one neutral particle must have been emitted and that the two-prong event V, seen in the spark chambers, with vertex pointing back toward A or B and which is consistent with the decay of a Λ^{o} or K^{o} could enable momentum to be balanced at B.

Of the three tracks of particles emerging from B, track 43 has been followed through the emulsion but is too oblique to have been detected in the spark chambers; track 42 passes through 3 mm of emulsion before interacting, producing a star with a single heavy prong; track 41 passes through the SD without undergoing appreciable deviation. Neither tracks 41 or 42 are produced by electrons.

B. Emulsion Measurements on Tracks Emerging from Vertex B

Ionization and multiple scattering measurements have been made in an attempt to identify the particles producing tracks 41, 42 and 43. An interval of about eight months between manufacture and development produced rather severe fading conditions which made it impossible to determine directly the "plateau" ionization blob density, b_o, in each plate. Using the favorable circumstance that the event itself contains seven tracks of near minimum ionization it was possible to estimate the relative ionization density b/b_o for each of them and using reasonable assumptions, to estimate b_o in each plate (~20 blobs per 100 μm).

The emulsions were processed off glass. Multiple scattering measurements were carried out on all the tracks from both vertices A and B of the event in eight plates and using a Koritska MS_2 microscope. Typical magnitudes of 50 μm were obtained for the distortion vector. Only C distortion was observed. Third differences were used to estimate the scattering for each track and yielded a uniform sample of data despite the quite different distortion corrections needed from plate to plate and track to track.

C) Particle Identification

Despite the careful measurements it was not possible to identify the particles unambiguously. Particles 41 and 42 could be identified either as π or μ while particle 43 could be K, π or μ. Particle 3 from the primary interaction could be almost anything

but it is the only one with both sufficient energy and with direction of motion through the spark chamber system compatible with the particle that registered in the muon identifier.

The tracks W_1, S_1 seen in the spark chambers are interpreted as due to a V^o decay.(*) The V^o opening angle and the angle between the directions of W_1 and the flight direction of the neutral particle producing it, together with the observation that S_1 passes through 47 g cm^{-2} of lead in the SD restricts the ranges of V^o momenta to 1.9 - 2.5 GeV/c for a Λ^o and 1.7 - 2.4 GeV/c for a K^o. The corresponding flight times would then range between 2.0 to 2.7 times the mean life for a Λ^o and 2.7 to 3.8 times for a K^o.

D. Interpretation of Vertex B as a Decay

Assuming vertex B represents a decay the chance of any known decay process (not involving decay of a charmed particle or heavy lepton) occurring within 182 μm of the interaction is at most 10^{-6}.

Owing to ambiguities in identification of the particles whose tracks are seen and the possible presence of unseen neutral particles, it is impossible to get an unambiguous intepretation of the

---

(*) Since the intersection point of W_1, S_1, is near the Al plate separating the two gaps of the WG spark chamber their interpretations in terms of a neutron interaction cannot be entirely excluded. Since the plate is only 3 mm thick, the two tracks are coplanar with A or B and consistent with interpretation in terms of Λ^o or K^o decay, the alternative interpretation as a neutron interaction is very unlikely. It cannot be established whether the neutral particle involved comes from A or B. Its association with B would greatly increase the likelihood of that vertex representing the decay of a hsort-lived charmed particle.

event. Even allowing for the inaccuracies of the scattering and ionization measurements, interpretation in terms of the observed charmed baryon decay mode,[4] $\Lambda_c^{\pm}$ (2.25 GeV) $\rightarrow {}^{o}\pi^{+}\pi^{-}\pi^{\pm}$, gives a mass discrepancy of at least two standard deviations; while interpretation in terms of the charmed meson mode, $D^{\pm}$ (1.87 GeV) $\rightarrow K^{o}\pi^{+}\pi^{-}\pi^{\pm}$, gives a mass discrepancy of more than three standard deviations. On the other hand, assuming the emission of unseen neutral particles a large number of interpretations is possible, including

$$\Lambda_c^{\pm} \text{ (2.25 GeV)} \rightarrow \pi^{\pm}\pi^{\pm}\pi^{\mp}\pi^{o}; \; D \text{ (1.87 GeV)} \rightarrow K^{o}\pi^{\pm}\pi^{\pm}\pi^{\mp}\pi^{o}.$$

Interpretation in terms of either charmed particle or heavy lepton decay with one of the particles a muon is also possible.

There is clearly little point in speculating further. To sum up, the most likely interpretation seems to be in terms of the production of an unstable particle that decays 6×10^{-13} s after emission from a neutrino interaction. If the apparent V^{o} decay is associated with vertex B its interpretation as a charmed particle decay would have a very high probability. If the V^{o} decay is not associated with vertex B there is a chance of ~ 1 in 400 of the vertex B arising from the interaction of a hadron emitted from the ν interaction. Only one likely short-lived decay particle with lifetime in the range 2×10^{-14} s to 6×10^{-11} s has been observed in 37 ν interactions.

VIII. THE VIABILITY OF EMULSION HYBRID TECHNIQUES

The present experiment has demonstrated that the hybrid technique can be used successfully to locate high energy ν interactions in nuclear emulsion. It has underlined the importance of using in the vertex prediction fast secondary particles that undergo only small multiple scattering. The success rate for locating interactions with two secondaries of momentum $\gtrsim$ 500 MeV/c was five times greater than for interactions with none. Two thirds of the events were located in searching an area of 10 cm^2 of emulsion pellicle, or less, while no event located required a search of more than 34 cm^2. Throughout the collaboration 18 scanners found events at a rate of rather less than one event per week. If a more effective method of secondary momentum analysis had been available the search could have been confined to considerably fewer events without appreciably reducing the overall number of events located.

Some other important factors that should be taken into account in the design of hybrid emulsion experiments include

(a) The effect of multiple scattering in increasing the search volume. Material between the secondary particle detector and the emulsion should be reduced to a minimum and confined to material of low atomic number. Multiple scattering in the emulsion stack limits the desirable thickness of the emulsion in the beam direction.

(b) The presence of electrons among the tracks of secondaries used

for vertex production introduces ambiguities since electron pairs will in general diverge from a secondary vertex.

(c) The distance R between detector and emulsion should be kept small. The magnitude of the search volume is approximately proportional to the parameter $(\alpha R + \delta)^3$ where α is the angular uncertainty in direction and δ the lateral uncertainty in position of the tracks used for vertex reconstruction. It should be possible to reduce R drastically compared with its value in this experiment.

Nevertheless the present experiment was something of a pioneering experiment in its field. It has accomplished its main purpose by locating 37 ν interactions in emulsion and by uncovering among them the first candidate decay of a short-lived charmed particle in neutrino interactions and thus demonstrating the viability of the technique.

ACKNOWLEDGEMENTS

We wish to thank the Director of Fermilab, Professor R. R. Wilson, for his encouragement and support, and very many members of the Fermilab staff for their invaluable contributions towards the implementation of this experiment.

Preliminary tests as well as the processing of the emulsion were carried out at CERN and we are indebted to the Directors-General and many members of CERN staff, especially O. Mendola and the late Max Roberts, for their very considerable contributions.

We wish to thank C. Bernardini and L. Voyvodic for contributions in the early stages of the preparation of this experiment, D. Petersen for his assistance during part of the run and M. Bertino for his essential technical assistance in the preparation and running of the experiment, as well as to the many other technical personnel from many laboratories, especially the scanners without whose careful and patient work the experiment would have been impossible. Finally we are indebted to colleagues, too numerous to mention by name, from each of the participating laboratories, who have helped greatly in discussions and in many other ways.

REFERENCES

[1] See review of the situation with full set of references given by F. A. Nezrick in a talk at the Triangle Seminar on Recent Developments in High Energy Physics, Campione d'Italia, Oct. 1977 (Fermilab Report Conf. 77/112 Exp.).

[2] E. H. S. Burhop, W. Busza, D. H. David, B. G. Duff, D. A. Garbutt, F. F. Heymann, K. M. Potter, J. H. Wickens, C. Bricman, J. Lemonne, J. Sacton, G. Schorochoff, M. Roberts and W. Toner, Nuovo Cim. 39 (1965) 1037.

[3] E. H. S. Burhop, D. H. Davis, D. N. Tovee, D. Petersen, A. L. Read, G. Coremans-Bertrand, J. Sacton, P. Vilain, A. Breslin, A. Montwill, M. A. Roberts, D. A. Garbutt, F. R. Stannard, G. Blaes, R. Klein, F. M. Schmitt, G. Baroni, G. Ceradini, M. Conversi, L. Federici, M. L. Ferrer, S. Gentile, S. Di Liberto, S. Petrera, G. Romano, R. Santonico, G. Bassompierre, M. Jung, N. Kurtz, M. Paty and M. Schneegans, Phys. Lett. 65B, 299 (1976).

[4] B. Knapp, W. Lee, P. Leung, S. D. Smith, A. Wijanco, J. Knauer, D. Yount, J. Bronstein, R. Coleman, G. Gladding, M. Goodman, M. Gormley, R. Messner, T. O'Halloran, J. Sarracino, A. Wattenberg, M. Binkley, I. Gaines and J. Peoples, Phys. Rev. Lett. 37, 882 (1976).

TABLE I

Total Area Scanned and Events Found in

Different Areas of Plates in the z (beam) Direction

	Total	Zone 1	Zone 2	Zone 3	Zone 4
Range of z in mm from emulsion edge closest to WG spark chamber	0-73	0-18.25	18.25-36.5	36.5-54.75	54.75-73
Area scanned cm^2) [a]	3345	878	1005	891	571
No. of events found [b]	34	14	9	7	4
Area scanned per event found (cm^2)	95.6	62.7	111.7	127.3	142.8

[a] An area cut-off of 30 cm^2 for any single event has been applied in order to make the results from different laboratories comparable. This cut means that two events found after a scan greater than 30 cm^2 have been omitted from the table.

[b] The detailed area scan figures for one event were not available.

TABLE II

Dependence of Location Efficiency of Interactions in Emulsion on Presence of "straight" Tracks in the Shower Detector

	Total number of events[a]	Number of events with 0 "straight" tracks	1 "straight" track	$\geq$ 2 "straight" tracks
Vertex located	23	2	6	15
Vertex not located	115	36	37	42
Fraction of events located	0.16	0.05	0.14	0.26

[a] This analysis was possible on only a fraction of events because the NG chambers were not operating during the early part of the experiment.

FIGURE CAPTIONS

Fig. 1: Diagram illustrating the experimental arrangement; V, veto counter; C_o, NG spark chamber; E, six emulsion stacks on frame: S_o, scintillation counter; WG, wide gap spark chamber; SD, shower detector comprising scintillator counters S_{1-4}, NG, spark chambers C_{1-4} and lead plates L_{1-5}; M, muon identifier.

Fig. 2: Illustrating construction of WG spark chamber, its associated Marx generator and electromagnetic shielding.

Fig. 3: Typical photograph of an event (16/119) (direct view only). The first gap (WG1) of the WG was not operating with maximum efficiency when this photograph was taken so that not all the tracks are seen in WG1. Sparks in the narrow gap chambers (NGSD) of the SD are seen to line up with the tracks in WG2. The system of pairs of illuminated fiducial holes are seen to the left (above and below) of WG1. A chance oblique background track (unconnected with the event) is seen in the narrow gap veto chambers (NGV). The display (PH) records the integrated pulse height of the output from the photomultipliers of SD. The display (EMI) records the hodoscope pattern of the muon identifier.

The corresponding event seen in the emulsion has nine minimum ionization tracks emerging. Seven of these have directions agreeing within 2^o both in dip and

azimuth with the seven tracks seen in WG2. The other two tracks were outside the acceptance angle of the spark chamber.

Fig. 4: (a) Distribution of mean square dispersion of reconstructed points about fitted spark chamber tracks for a sample of 200 tracks.

(b) Displacement D between the reconstructed tracks in the two gaps due to opposite electric field directions in the gaps, plotted as a function of the projected angle between the tracks. The suffixes x, y refer to the two projection planes.

(c) Distribution of perpendicular distance between reconstructed vertex and tracks used in reconstruction.

Fig. 5: Illustrating the accuracy of vertex prediction. Distribution of quantities (a) Δx; (b) Δy; (c) Δz. The shaded area refers to the upper stacks, A, B, C, the unshaded area to the lower stacks, D, E, F.

Fig. 6: Illustrating the differences of angle of tracks in emulsion and WG spark chamber for events located for (a) azimuthal angle, θ; (b) dip angle, ϕ.

Fig. 7: Comparison of number distribution of minimum ionization tracks for events found in emulsion (shaded) and ν interactions in BEBC containing Ne - H_2 mixture. The two distributions are normalized for the same number of events with $n_s > 3$. The loss of events for small n_s in emulsion is clear.

Fig. 8: Distribution of search area of emulsion plates required to locate the 37 events found.

Fig. 9: Distribution of positions of events located in the x, z plane for each emulsion pellicle, illustrating the effect of multiple scattering in emulsion in reducing efficiency of finding events.

Fig. 10: Depth distribution of events located in emulsion pellicles (normalized to mean thickness of 60 μm), illustrating possible loss of events near the glass backing.

Fig. 11: Distribution of angles between ν beam direction and direction of emission of minimum ionization particles for ν interactions in nuclear emulsion.

Fig. 12: Prong-length distribution of black and grey prongs from the ν interactions located in nuclear emulsion. In addition to the prongs included in the distribution there were 19 prongs that left the stack distances ranging from 374 μm to 34.4 mm.

Fig. 13: Schematic drawing based on spark chamber photographs associated with event No. 8/151 which contains the short-lived charm candidate. The tracks seen in WG are shown by thick lines. Also shown is an enlarged view of the region around the interaction as seen in emulsion. Tracks 5, 43 seen in emulsion as well as S_1, seen in the NG chambers, are too oblique to have been seen in WG. The particle producing track 42 interacts before leaving the emulsion. Track 2 seen in emulsion, is not seen in the spark chamber although it might have been expected to be seen there.

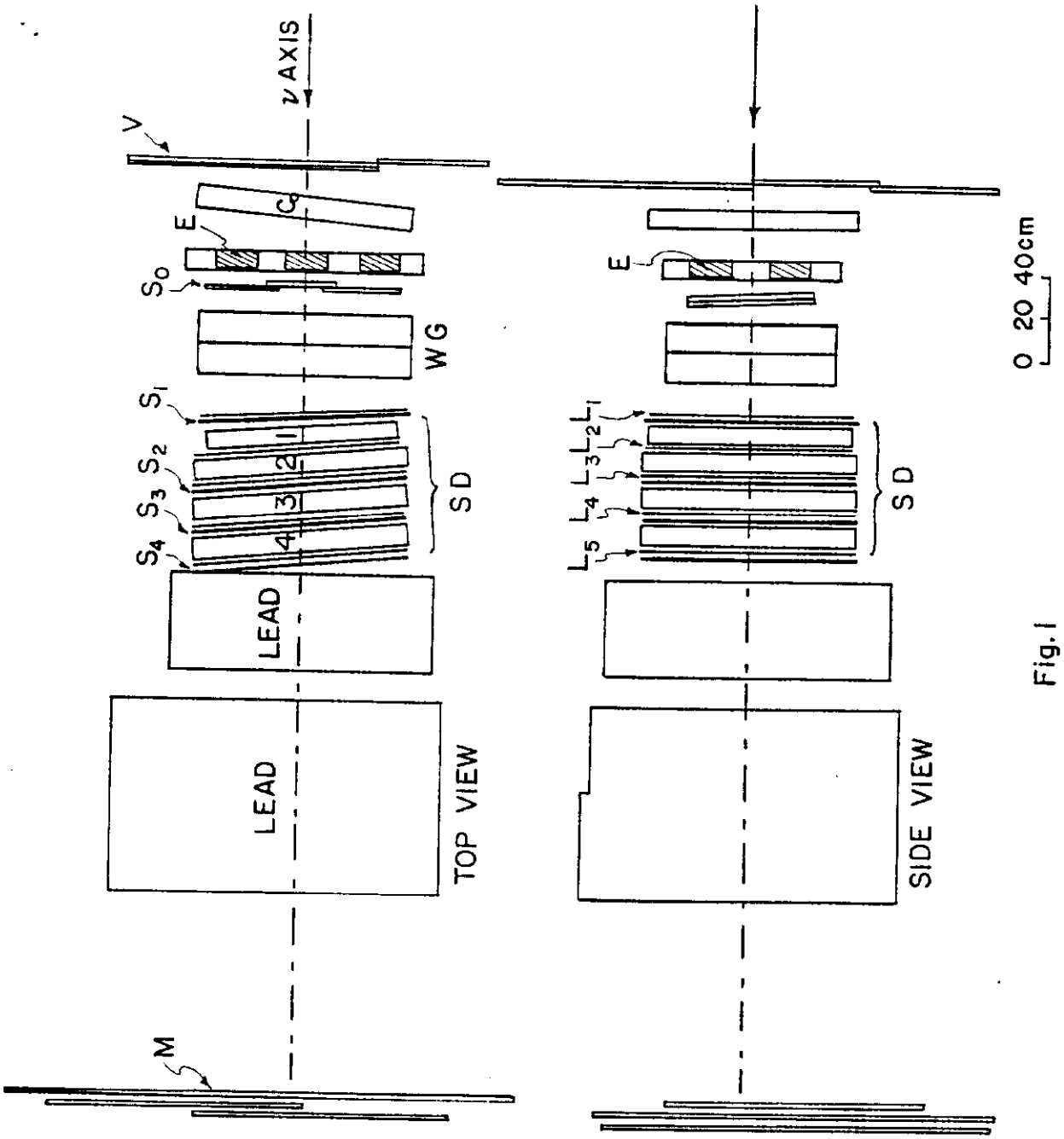
ν AXIS
V
C
E
S0
WG
S1
S2
S3
S4
1
2
3
4
SD
LEAD
LEAD
TOP VIEW
M
E
L1
L2
L3
L4
L5
SD
SIDE VIEW
0 20 40cm

Fig. 1

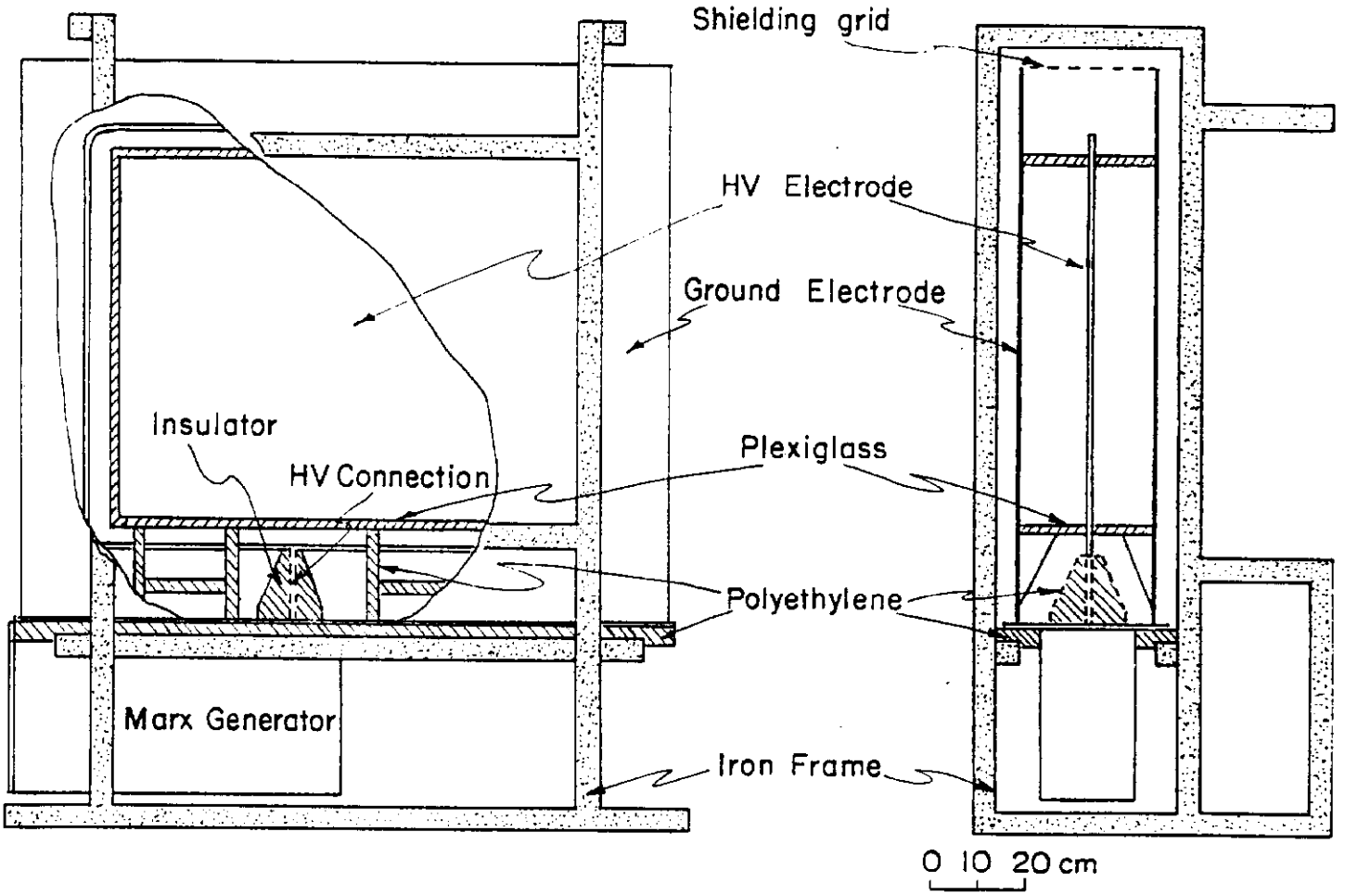
Shielding grid
HV Electrode
Ground Electrode
Insulator
HV Connection
Plexiglass
Polyethylene
Marx Generator
Iron Frame
0 10 20 cm

Fig. 2

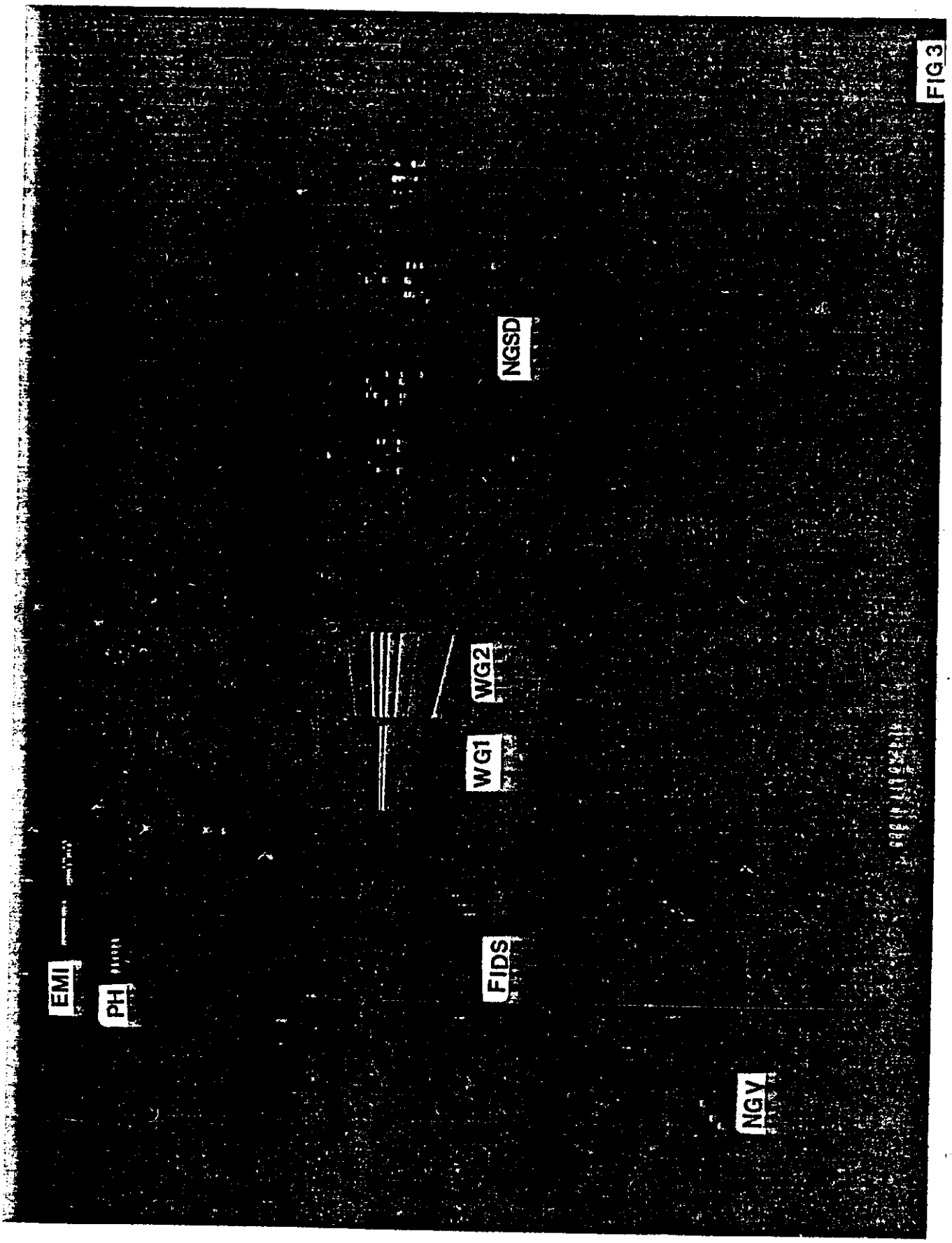

FIG3

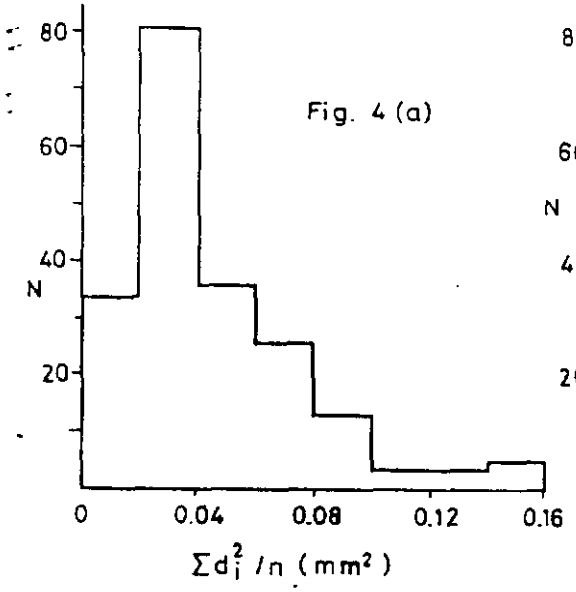

Fig. 4 (a)

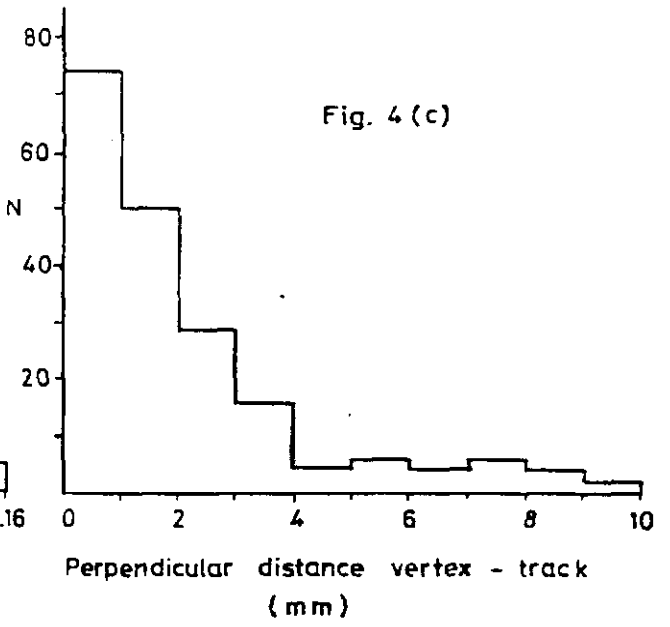

Fig. 4 (c)

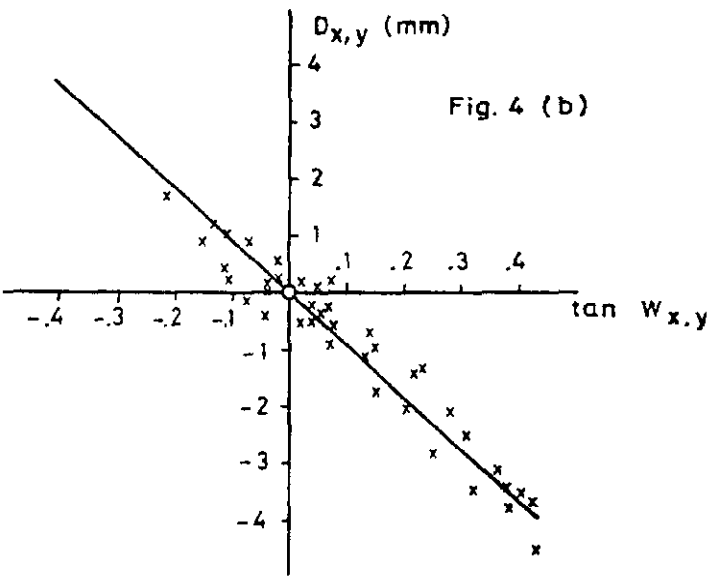

Fig. 4 (b)

225_795_4

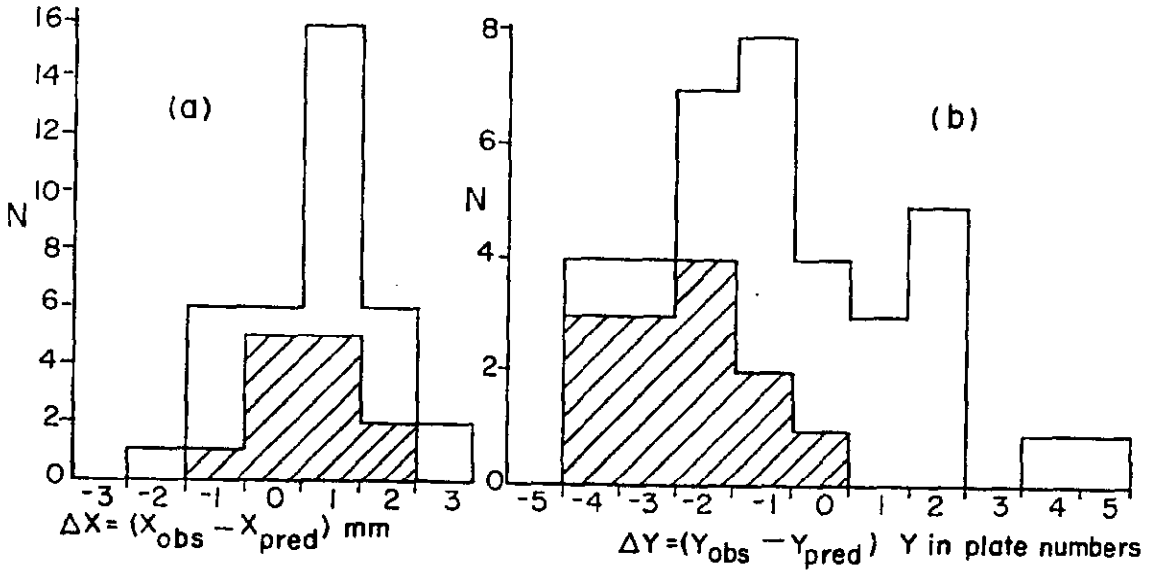
(a)
N
ΔX = (X obs − X pred) mm
(b)
N
ΔY = (Y obs − Y pred) Y in plate numbers

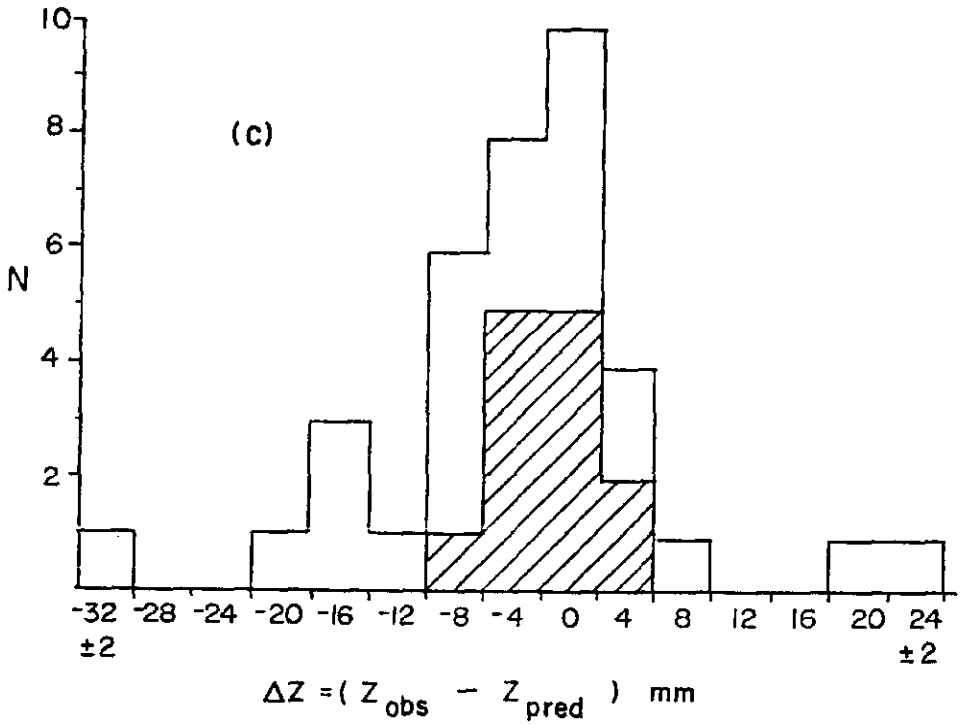
(c)
N
±2
±2
ΔZ = (Z obs − Z pred) mm

Fig. 5

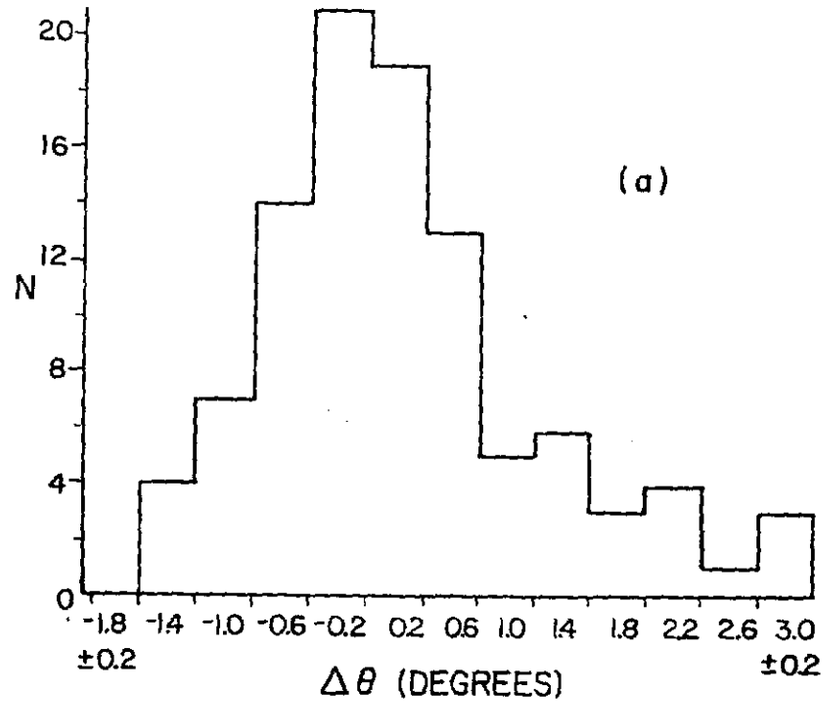
20
16
12
N
8
4
0
(a)
-1.8 -1.4 -1.0 -0.6 -0.2 0.2 0.6 1.0 1.4 1.8 2.2 2.6 3.0
±0.2
±0.2
Δθ (DEGREES)

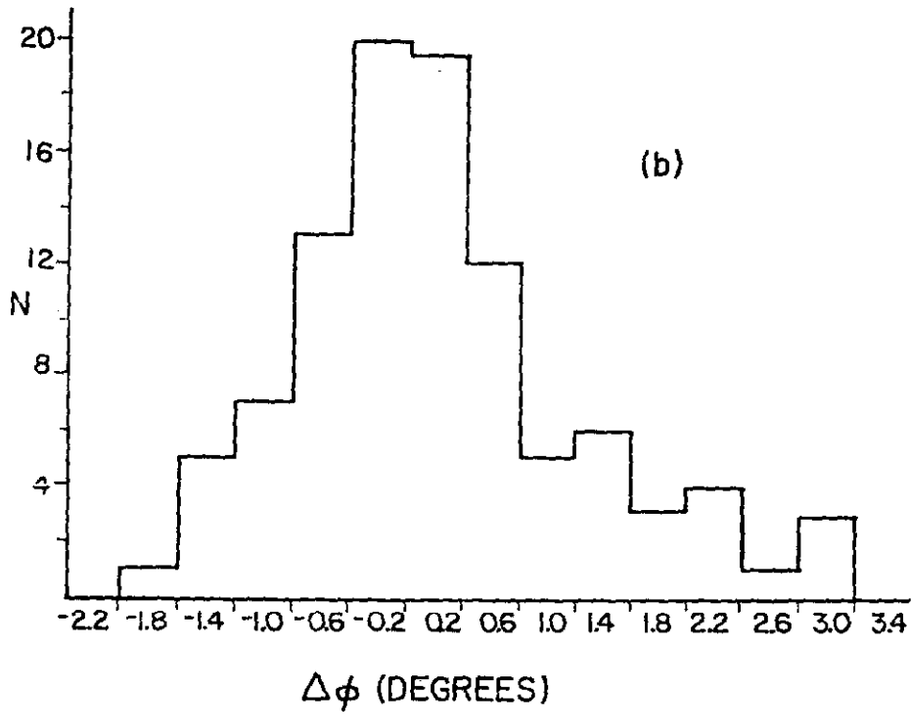
20
16
12
N
8
4
(b)
-2.2 -1.8 -1.4 -1.0 -0.6 -0.2 0.2 0.6 1.0 1.4 1.8 2.2 2.6 3.0 3.4
Δφ (DEGREES)

Fig.6

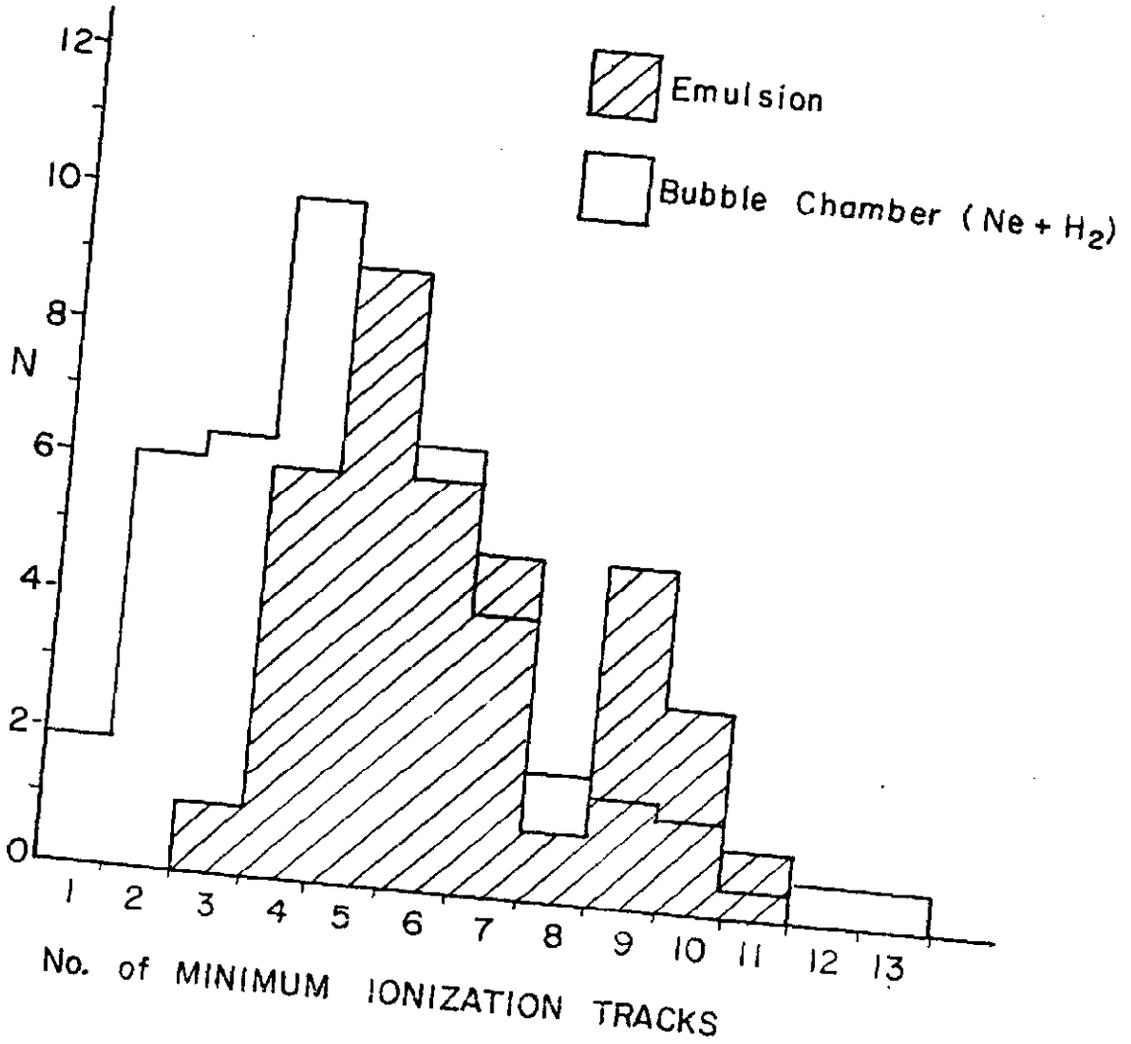
12
10
8
N
6
4
2
0
Emulsion
Bubble Chamber (Ne + H_2)
1 2 3 4 5 6 7 8 9 10 11 12 13
No. of MINIMUM IONIZATION TRACKS

Fig. 7

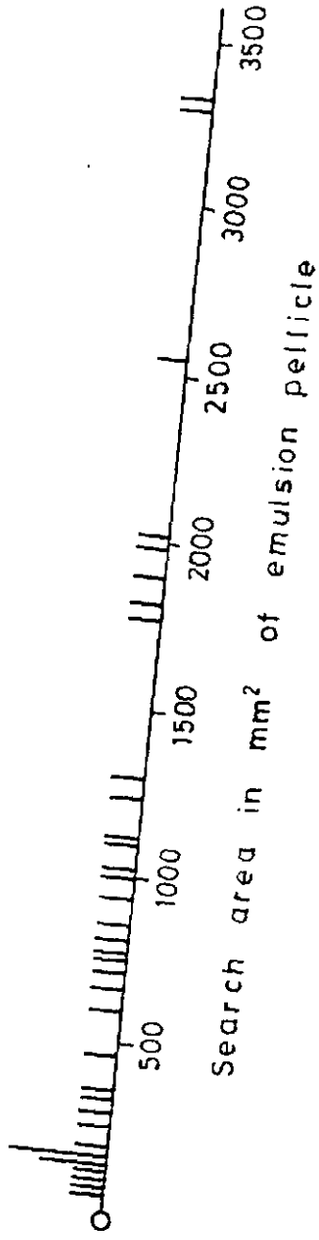
500
1000
1500
2000
2500
3000
3500
Search area in mm² of emulsion pellicle

Fig. 8

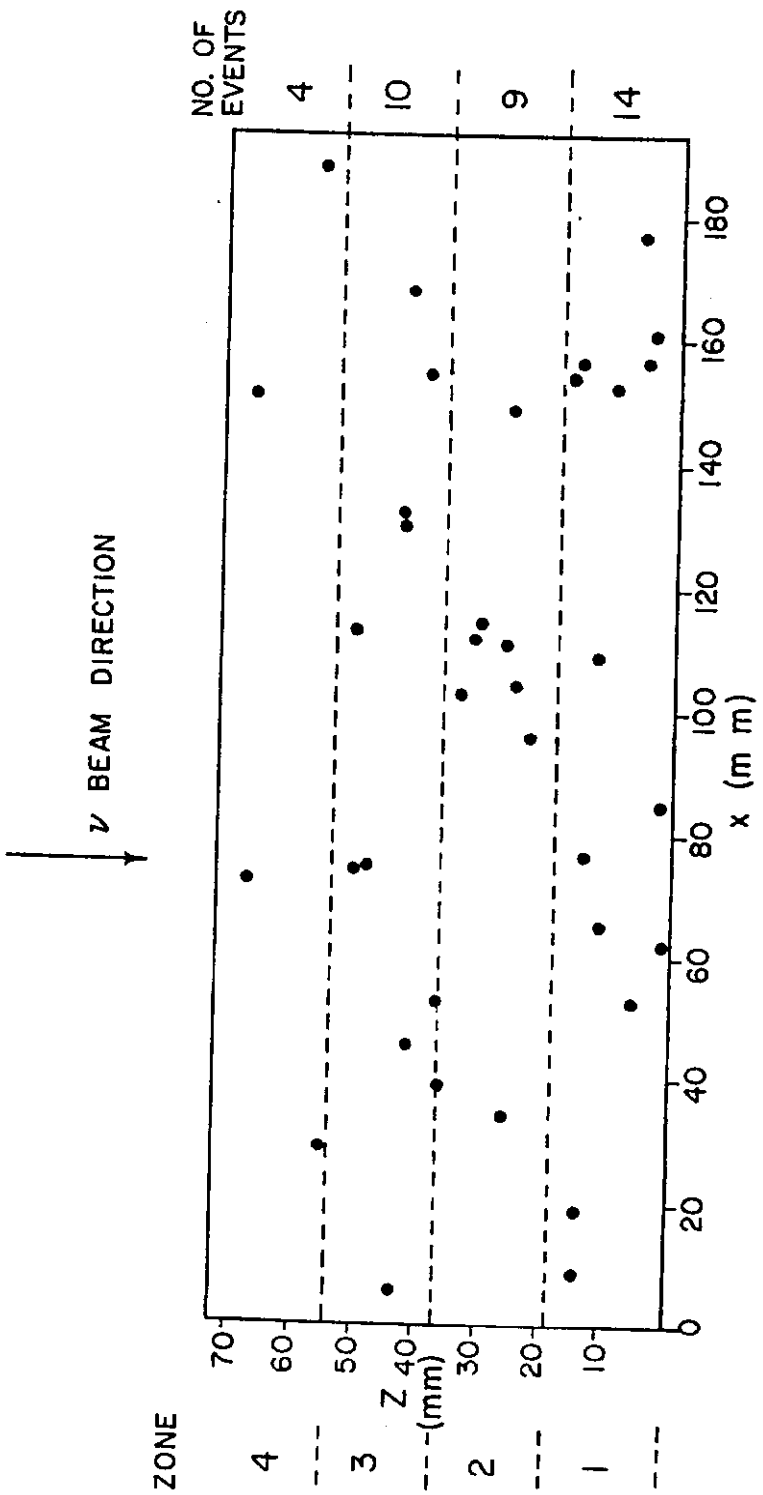
ν BEAM DIRECTION
NO. OF EVENTS
4
10
9
14
ZONE
4
3
2
1
Z (mm)
70
60
50
40
30
20
10
0
20
40
60
80
100
120
140
160
180
x (m m)

Fig. 9

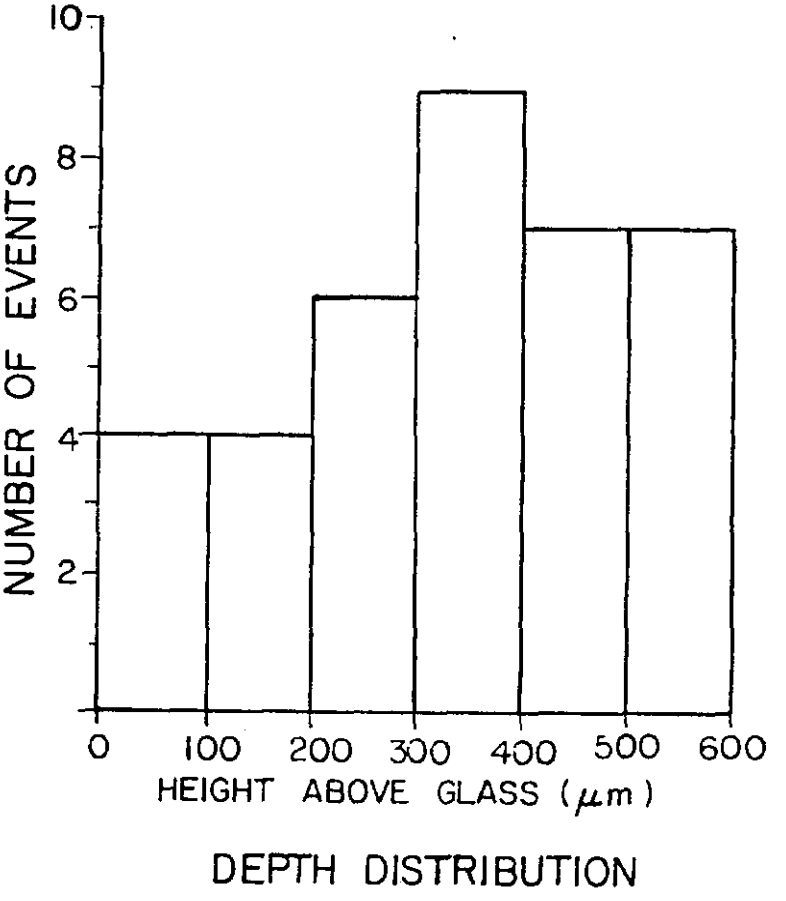
10
8
6
4
2
NUMBER OF EVENTS
0
100
200
300
400
500
600
HEIGHT ABOVE GLASS (μm)
DEPTH DISTRIBUTION

Fig.10

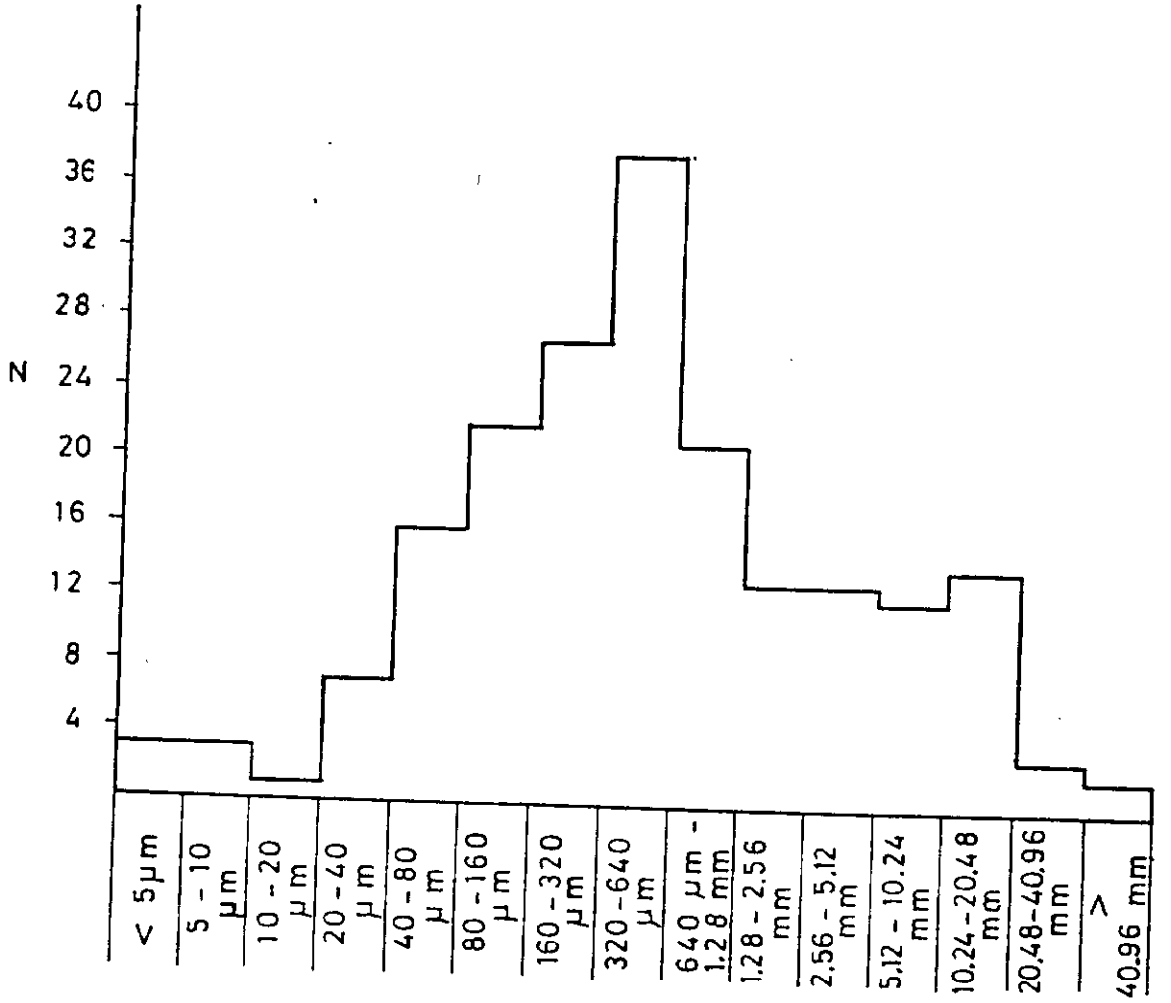
N
40
36
32
28
24
20
16
12
8
4
< 5µm
5 - 10 µm
10 - 20 µm
20 - 40 µm
40 - 80 µm
80 - 160 µm
160 - 320 µm
320 - 640 µm
640 µm - 1.28 mm
1.28 - 2.56 mm
2.56 - 5.12 mm
5.12 - 10.24 mm
10.24 - 20.48 mm
20.48 - 40.96 mm
> 40.96 mm
Length of prong

Fig. 12

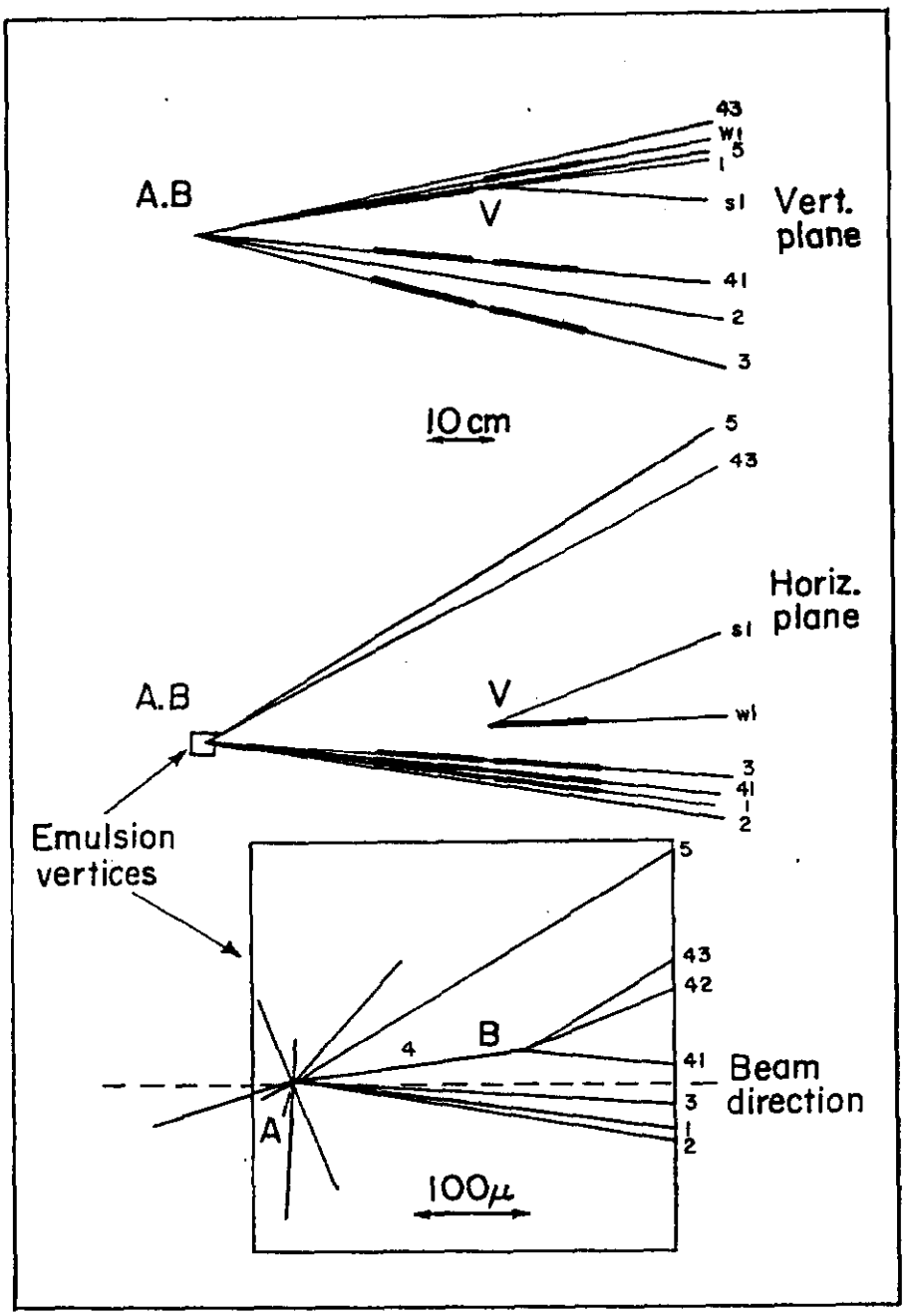
43
w1
5
1
A.B
V
s1
Vert.
plane
41
2
3
10 cm
5
43
Horiz.
plane
s1
A.B
V
w1
3
41
1
2
Emulsion
vertices
5
43
42
4
B
41
Beam
direction
3
A
1
2
100μ

Fig. 13